Protective Effect of Ginsenoside Rd on Military Aviation Noise-Induced Cochlear Hair Cell Damage

Xuemin Chen
Chinese PLA General Hospital https://orcid.org/0000-0003-0653-8752
Yu-hui LIU
Air force medical university
Shuai-fei JI
Chinese PLA general hospital
Xin-miao XUE
Chinese PLA General Hospital
Peng LIU
Chinese PLA General Hospital
Cong-cong LI
Air Force Medical University
Min ZHANG
Air Force Medical University
Yao-ming CHANG
Air Force Medical University
Xiao-cheng WANG (wxcnose@126.com)
The First Affiliated Hospital of Air Force Military Medical University,

Research

Keywords: ginsenoside Rd, noise-induced hearing loss, cochlea, oxidative stress, Sirtuin1

Posted Date: July 7th, 2021

DOI: https://doi.org/10.21203/rs.3.rs-673642/v1

Abstract

Background Soldiers are often exposed to high-intensity noise produced by military weapons and equipment during activities, and the incidence of noise-induced hearing loss (NIHL) in many arms is high. Oxidative stress has a significant role in the pathogenesis of NIHL, and research has confirmed that ginsenoside Rd (GSRd) suppresses oxidative stress. Therefore, we hypothesized that GSRd may attenuate NIHL and cochlear hair cell loss, induced by military aviation noise stimulation, through the Sirtuin1/proliferator-activated receptor-gamma coactivator 1α (SIRT1/PGC-1α) signaling pathway.

Methods Forty-eight male guinea pigs were randomly divided into four groups: control, noise stimulation, GSRd, and glycerol. The experimental groups received military helicopter noise stimulation at 115 dB (A) for 4 h daily for five consecutive days. Hair cell damage was evaluated by using inner ear basilar membrane preparation and scanning electron microscopy. Terminal dUTP nick end labeling and immunofluorescence staining were conducted. Changes in the SIRT1/PGC-1α signaling pathway and other apoptosis-related markers in the cochleae, as well as oxidative stress parameters were used as readouts.

Results Loss of outer hair cells, more disordered cilia, prominent apoptosis, and elevated free radical levels were observed in the experimental groups. GSRd treatment markedly improved morphological changes and apoptosis through decreasing Bcl-2 associated X protein (Bax) expression and increasing Bcl-2 expression. In addition, GSRd upregulated superoxide dismutase (SOD) and glutathione peroxidase (GSH-Px) levels, decreased malondialdehyde (MDA) levels, and enhanced the activity of SIRT1 and PGC-1α messenger ribonucleic acid and protein expression.

Conclusion GSRd can improve structural and functional damage to the cochleae caused by noise. The underlying mechanisms may be associated with the SIRT1/PGC-1α signaling pathway.

Introduction

Noise-induced hearing loss (NIHL) is a type of sensorineural hearing loss caused by overexposure to occupational or recreational noise. It can seriously affect a person's quality of life and results in immense economic loss [1]. Soldiers are often exposed to high-intensity noise produced by military weapons and equipment during training and combat activities, and the incidence of NIHL is high in many arms such as artillery, armored troops, aviation units, and warship units. The noise sources in a military operating environment are primarily the engines of aircraft, tanks, warships and other weapons, and the means of delivery such as the firing of guns and gunpowder explosion. The noise sources in a military helicopter are primarily produced by blade rotation, impulse noise generated by high-speed advance, compressor noise, and exhaust noise produced by engine driving, etc., which are broadband noises but primarily composed of low-frequency components. The noise of a military helicopter is harmful to the human body, but the exploration of its degree of damage, characteristics, mechanism, and protection is not sufficiently comprehensive.

Considerable efforts exist to elucidate the pathogenesis of NIHL. However, the mechanisms underlying NIHL are not completely understood. The current belief is that the causes of NIHL include environmental and genetic factors. Environmental factors include noise intensity, spectrum characteristics, and the length of time of exposure to noise. Genetic factors primarily refer to NIHL-related susceptibility genes such as *CDH23* [2], *CASP3* [3], *GRM7* [4], and *GJB2* [5]. Three main theories related to mechanical damage, metabolic damage, and vascular changes explain the pathogenesis of NIHL [6–8]. Increasing evidence indicates the possible role of dysregulation of free radicals and oxidative stress [9–11]. Oxidative stress is an imbalance between cell damage and cell adaptive changes that result from reactive oxygen species (ROS). The excessive production of ROS may be a major cause of NIHL, and antioxidants have a protective role against NIHL [12].

Critical to the homeostasis of redox systems is Sirtuin 1 (SIRT1), a nicotinamide adenine dinucleotide (NAD)-dependent histone deacetylase and member of the SIRT family. SIRT1 deacetylates certain substrates, including proliferator-activated receptor-gamma coactivator 1α (PGC-1α), class O of fork head box (FoxO), p53, and Nrf2 [13–17]. PGC-1α is a main regulator influencing the expression of several mitochondrial genes, thereby making a valuable contribution toward mitochondrial biogenesis [18]. Mitochondrial dysfunction may result in oxidative stress, which contributes to the pathogenesis of NIHL and possibly influences SIRT1 and numerous cellular antioxidant defense mechanisms [12, 19]. In response to oxidative stress, SIRT1 is redistributed at the chromatin level, and causes deregulation at the transcription level [20].

SIRT1 has a protective role against cochlear injury in age-related hearing loss (AHL) [21, 22], which is another type of sensorineural hearing loss that has a similar pathogenesis as NIHL. In vitro, inhibition of SIRT1 expression also increases the apoptosis rate of House Ear Institute-Organ of Corti 1 (HEI-OC1) inner ear cells, which suggests that SIRT1 has a role in the pathogenesis of AHL [23], as well as in protecting against NIHL [24].

Ginsenoside Rd (GSRd), a constituent of ginseng that has many therapeutic benefits, has also been shown to suppress oxidative stress [25–31]. In this study, we tested our hypothesis that GSRd supplementation may attenuate NIHL via the regulation of oxidative stress and apoptosis, mediated by the SIRT1/ PGC-1α signaling pathway.

Methods

Functional enrichment analyses of GSRd and SIRT1 via bioinformatics analyses

We retrieved essential information of GSRd from the *Encyclopedia of Traditional Chinese Medicine* (*ETCM*) [32]. The gene ontology (GO) enrichment analysis of GSRd pharmacological effects and the single gene enrichment analysis of SIRT1 were conducted by using the STITCH database [33].

Animal groups

Forty-eight male guinea pigs, weighing approximately 250–300 g, were purchased from the Experimental Animal Center of Air Force Medical University (Xi'an, China). All animals had a sensitive auricle reflex, normal tympanic membrane, and no history of noise contact. They were housed in an environment with natural light, room temperature of 20–25ºC, air relative humidity of 60–65%, and free access to food and water. Adaptive feeding was administered for 5 d before the start of the experiment. All experimental procedures were approved by the Animal Ethics Committee of our university. Ginsenoside Rd (Tai-He Biopharmaceutical, Guangzhou, China) was kindly provided by the Department of Neurology in Xijing Hospital (Xi'an, China).

Guinea pigs were randomly assigned to one of four groups, each containing 12 animals: the control group (Con), which received no noise stimulation nor treatment; the noise group (NE), which was exposed to military helicopter noise but did not receive drug treatment; the GSRd treatment group (Rd), which was exposed to military helicopter noise and injected intraperitoneally with 30 mg/kg GSRd dissolved in glycerol; and the experimental control group (Vehl), which was exposed to military helicopter noise and injected intraperitoneally with just glycerol at 30 mg/kg. GSRd/glycerol was injected from 5 days before noise stimulation to the end of noise stimulation for a total of 10 days.

Noise stimulation and procedures

The ambient noise of a military helicopter was collected and input to a speaker (Soundtop SF-12; Jia-sheng Audio Equipment, Co., Ltd., Guangzhou, China) through a power amplifier (Soundtop QA-700; Jia-sheng Audio Equipment) for cyclic playback. Noise stimulation was conducted in a soundproof room with an air-conditioned fan to moisten the air and strengthen local ventilation. The guinea pigs from the experimental groups were placed in a rat cage on which a speaker was placed. The noise intensity was measured by an A-weighted sound level (Heng-sheng Electronics, Jiaxing, China) to ensure that the difference in the sound pressure level in the activity range of guinea pigs was less than 3 dB. The animals were exposed to 115 dB (A) noise stimulation for 4 hours daily for 5 consecutive days [34]. The Con group was not exposed to noise stimulation. The background noise in the cage was less than 20 dB, and the other conditions were the same as those in the experimental groups.

Tissue preparation

After detecting the hearing threshold levels [35], the animals were euthanized. The bilateral temporal bones of guinea pigs were removed, and the bilateral cochleae were separated immediately. There were 24 cochlear specimens in each group of guinea pigs. The specimens were distributed as shown in Table 2.

The cochlear tissues used in the surface preparation of the basilar membrane and section staining were removed and then soaked in 4% paraformaldehyde, and those used for scanning electron microscopy (SEM) were soaked in 2.5% glutaraldehyde. The stapes were removed with microscopic forceps under an anatomical microscope. A small hole was created at the tip of the cochlea by a syringe needle. The corresponding fixed fluid was slowly injected into the cochlea through the perforated cochlear tip and the

oval window more than three times. The specimens were then transferred into an Eppendorf tube containing the fixed solution overnight at 4ºC. Beginning on the second day, the 10% EDTA solution was replaced for decalcification for 14 days. The freshly decalcified solution was replaced every day until the cochlear bone softened. The decalcified cochlear tissues were used for surface preparation of the basilar membrane or were embedded in paraffin to prepare 5 μm sections parallel to the direction of the modiolus for terminal dUTP nick end labeling (TUNEL) and immunofluorescence staining. The rest of the specimens were stored at -80ºC.

Phalloidin staining

Phalloidin staining was conducted, as described by Qi and colleagues [36]. The spiral case and spiral ligament were removed with microscopic forceps under an anatomical microscope. The basilar membrane was separated step-by-step from the tip to the bottom of the cochlea and was moved into a 96-well plate. The removed basilar membranes were rinsed three times with 0.1M phosphate-buffered saline (PBS) for 1 min each time. A 100 μL of 1% Triton X-100 (MP Biomedicals, Solon, OH, USA) was subsequently added to each hole for 10 min. Specimens were rinsed three times with 0.1M PBS for 5 min each time. A phalloidin dilution (1:1000; ab176753; Abcam, Cambridge, MA, USA) was added to each well for 30 min without light. The specimens were rinsed three times with 0.1M PBS and 4,6-diamino-2-phenylindole (DAPI) (1:1000; ab104139; Abcam) and staining was conducted for 8 min without light to display the nucleus. The specimens were then rinsed with 0.1M PBS three times for 5 min each time. The basilar membrane was drawn onto the glass slide by using a pipette. The positive and negative sides of the basilar membrane were observed under a microscope (SMZ745; Nikon Corporation, Tokyo, Japan). The slides were carefully covered with an 80% glycerin seal to prevent fluorescence quenching. A confocal microscope (LSM 800; Zeiss, Oberkochen, Germany) was used to observe the experimental results.

SEM observation

The experimental steps of SEM corresponded to those proposed in articles by Sung et al. [37] and Santi et al. [38]. The basilar membrane was soaked overnight in 2.5% glutaraldehyde at 4ºC. The specimens were rinsed three times with 0.1M PBS for 15 min each, and then postfixed in 1% osmium tetroxide for 2 h at a room temperature of 20°C–25°C. The specimens were then dehydrated with 30%, 50%, 70%, 80%, and 90% gradient ethanol and anhydrous ethanol; critical-point-dried by using liquid carbon dioxide; and then sputter-coated with gold-palladium for 30 s. The results were observed under a scanning electron microscope (S-3400; Hitachi, Tokyo, Japan).

TUNEL staining

TUNEL staining, as described by Liu and colleagues [39], was carried out on sections of the cochlea by using the *In Situ* Cell Death Detection Kit (11684795910; Roche, Basel, Switzerland), based on the manufacturer's instructions. Sections of the cochlea were deparaffinized using xylene, hydrated with anhydrous, 90%, 80%, and 70% gradient ethanol. After rinsing with distilled water, the sections were

covered with proteinase K solution for 15 min. They were subsequently rinsed with 0.1M PBS and distilled water for 6 min each and fixed with 3% methanol-hydrogen peroxide solution for 20 min. Following three rinses with 0.1M PBS for 6 min each, the sections were covered with 3% bovine serum albumin-PBS solution for blocking, followed by incubation with the TUNEL reaction mixture in the dark for 1 h at a room temperature of 20°C–25°C. Finally, the sections were rinsed with PBS-Tween (PBST) buffer solution and 0.1M PBS for 6 min each. The results were examined and photographed under fluorescence microscopy (DP71; Olympus, Tokyo, Japan).

Immunofluorescence staining for 4-hydroxy-4-hydroxynonenal and 3-nitrotyrosine

Immunofluorescence staining was carried out, as described by Tian and colleagues [40]. Sections of cochlea were deparaffinized using xylene; hydrated with anhydrous, 90%, 80%, and 70% gradient ethanol; and then rinsed three times with 0.1M PBS for 10 min each. A 1% Triton X-100 (MP Biomedicals) was added for 10 min. Three rinses were carried out using 0.1M PBS. The sections were incubated with 5% BSA (MP Biomedicals) for 1 h. The antibodies used for immunofluorescence staining included rabbit polyclonal anti-4-hydroxy-4-hydroxynonenal (anti-4-HNE) (1:1000; ab46545; Abcam) and mouse monoclonal anti-3-nitrotyrosine (anti-3-NT) (1:1000; ab61392; Abcam). Antibodies were diluted and were added to the sections. The sections were placed in a black wet box and stored overnight in a refrigerator at 4ºC. They were removed on the second day and reheated at a room temperature of 20°C–25ºC for 1 h before the three washes with 0.1M PBS. The secondary antibodies of cy3-labeled goat antirabbit immunoglobulin G (IgG) (red, 1:1000; Zhuangzhi Biotechnology, Xi'an, China) and 488-labeled goat anti-mouse IgG (green, 1:1000; Zhuangzhi Biotechnology) were added and the sections were incubated at room temperature at 20°C–25°C without light for 2 h. Another three rinses with 0.1 M PBS were applied and 8 min of DAPI (1:1000, ab104139, Abcam, USA) staining was applied without light to display the nucleus. Glycerin (80%) was used to prevent fluorescence quenching. A confocal microscope (LSM 800; Zeiss) was used for observation.

Quantitative real-time polymerase chain reaction analysis

The protocols used in this study were conducted, as described by Chen et al [35]. RNAiso (TaKaRa, Kyoto, Japan) was added to the homogenized cochlear specimens to extract total ribonucleic acid (RNA), based on the manufacturer's instructions. The extracted RNA was diluted to 300–500 ng/μL, and then combined with 2 μL 5 × Primer Script RT Master Mix (TaKaRa). The 10 μL reverse transcription reaction system was filled with diethyl pyrocarbonate water. The mixture was placed in a real-time system (Applied Biosystems, Waltham, MA, USA) at 37ºC for 15 min and then at 85ºC for 5 s to synthesize the complementary DNA (cDNA) template. Two microliters of the cDNA template were mixed with 20 μL of SYBR Premix Ex Taq™ II (2×) (TaKaRa), 14 μL of diethyl pyrocarbonate water, and 2 μL of the forward and reverse primers (Table 3; Sangon, China). The configured reaction system was fully blown and mixed and then was added to an octagonal tube with 9 μL per hole. The parameters were set as follows: 95ºC for 30 s, 40 cycles of 95ºC for 5 s and 60ºC for 34 s, and 65ºC for 15 s. Glyceraldehyde-3-phosphate

dehydrogenase was used as an internal control and the $2^{-\Delta\Delta Ct}$ method was used to calculate the relative expression of the target gene.

Western blot analysis

The protocols used in this study were conducted as described by Su et al [41]. The left and right cochlea of the same guinea pig were placed together in a tissue homogenizer. A 200 μL protein extraction reagent (78505; Thermo Scientific, Waltham, MA, USA) containing 2mM phenylmethylsulfonyl fluoride was used as the protein lysate to extract the total cochlear proteins. The total protein concentration was calculated using the BCA Protein Assay Kit (23250; Thermo Scientific). A total of 30 μg of each protein sample was denatured, separated on 4–12% Bis-Tris PAGE gels, and then transferred to polyvinylidene fluoride membranes (0.45 μm; Millipore, Darmstadt, Germany). The membranes were blocked in 5% fat-free milk powder for 2 h at a room temperature of 20°C–25°C and were then incubated with rabbit polyclonal antibody against Bax (1:500; WL01637; Wanleibio, Shenyang, China), Bcl-2 (1:500; WL01556; Wanleibio, China), SIRT1 (1:500; WL02995; Wanleibio), PGC-1α (1:500; WL02123; Wanleibio), or β-actin (1:1000; WL01845; Wanleibio) overnight at 4ºC. After six rinses with PBST for 5 min each, the membranes were incubated in PBST with horseradish peroxidase-conjugated goat antirabbit IgG (1:5000; WLA023; Wanleibio) for 1 h at a room temperature of 20°C–25°C and were detected using enhanced chemiluminescence detection reagents (Millipore) in a Gel Image Analyzing System (Tanon Science & Technology, Shanghai, China). The band intensity was measured using Image J v1.51 (National Institutes of Health, Bethesda, MD, USA), and the values were normalized to β-actin.

Detection of superoxide dismutase activity, malondialdehyde level, and glutathione peroxidase level

The left and right cochlea of the same guinea pig were placed in the same Eppendorf tube, and the samples were prepared with 0.9% normal saline as a 10% homogenate. Superoxide dismutase (SOD) assay kit (WST-1 method; A001-3; Jiancheng Biotechnology, Nanjing, China), malondialdehyde (MDA) assay kit (TBA method; A003-1; Jiancheng Biotechnology), and glutathione peroxidase (GSH-Px) assay kit (colorimetric method; A005-1; Jiancheng Biotechnology) were used to detect SOD activity, MDA levels, and GSH-Px levels, based on the manufacturer's instructions. Each group's chromaticity was assessed using a microplate reader (Thermo Fisher) at 450 nm for SOD activity, 532 nm for the MDA level, and 412 nm for the GSH-Px level.

Statistical analysis

The results are presented as mean ± the standard error. The hearing level; immunofluorescence staining results; mRNA and protein expression; and SOD, MDA, and GSH-Px activities were statistically analyzed using one-way analysis of variance. Dunnett's t-test was used to compare the experimental and control groups. Differences were significant when $P < 0.05$. Statistical analyses were performed using GraphPad Prism 7.0 (GraphPad Software, San Diego, CA, USA) and SPSS 23.0 (IBM Corporation, Armonk, NY, USA).

Results

GSRd improved noise-induced hearing loss through the SIRT1/PGC-1α signaling pathway

The retrieval results in the ETCM database suggest that the diseases treated with GSRd include sensorineural hearing impairment, progressive sensorineural hearing impairment, and dysregulation of apoptosis (http://www.tcmip.cn/ETCM/index.php/Home/Index/cf_details. *html?id = 4640*). Therefore, we initially hypothesized that GSRd may be a candidate drug for hearing impairment. In addition, GO enrichment analysis showed that the pharmacological effects of GSRd are primarily the regulation of oxidative stress and apoptosis and involvement in mitochondrial activity **(Fig. 1)**. NIHL is a type of illness characterized by oxidative stress damage and apoptosis progression [42]. Previous results have demonstrated that GSRd can significantly reverse the increase in the auditory brainstem response threshold caused by noise stimulation **(Supplementary Fig. 1)** [35], which supports our initial hypothesis. The results of the GSRd GO enrichment analysis focused our attention on a molecule associated with the regulation of mitochondrial activity and oxidative stress, which is SIRT1 **(**Table 1**)**. Furthermore, SIRT1 single gene enrichment analysis demonstrated that the SIRT1/PGC-1α signaling pathway is more prominently involved in gene expression, oxidative stress, and apoptosis regulation.

GSRd ameliorated damage to cochlear hair cells of guinea pigs

The cochlear basilar membrane preparation and SEM were used to observe morphological changes of the hair cells in the inner ear of guinea pigs after noise stimulation. Basilar membrane phalloidin staining (**Fig. 2A**) revealed the microfilament cytoskeleton and manifested the distribution of actin in the cochleae. In the control group (Con), the outer hair cells of the guinea pigs were intact and neatly arranged, and the cilia were clearly visible and arranged in a "V" shape. The outer hair cells of the noise group (NE) and the experimental control group (Vehl) showed damage with different degrees of dot deletion. The degree of outer hair cell loss in the Rd treatment (Rd) group was less than that of the NE and Vehl groups.

SEM images (**Fig. 2B**) showed the structural damage to the cilia and supporting cells of inner ear hair cells. The SEM images of the Con group verified the results of phalloidin staining. In the NE and Vehl groups, the polarity of the outer hair cells disappeared, and the arrangement was disordered with lodging, fusion, and even falling off. Among them, the third layer of outer hair cells was most seriously damaged. Following Rd treatment, the outer hair cells in the Rd group showed slight lodging and loss of cilia.

Effect of GSRd on the expression of apoptotic factors in the cochleae of guinea pigs

The results of the terminal deoxynucleotidyl transferase-mediated dUTP-biotin nick end labeling assay (TUNEL) staining showed no TUNEL-positive cells in the cochleae of guinea pigs in the Con group. The NE and Vehl groups had TUNEL-positive cells, primarily distributed in the organ of Corti, vascular stria, and spiral ligament. The number of TUNEL-positive cells in the Rd group was lower than that in the NE and Vehl groups. The results of TUNEL staining are shown in **Fig. 2C.**

The results of quantitative real-time PCR (RT-qPCR) and western blot analysis showed that the levels of B-cell lymphoma-2 (Bcl-2)-associated X protein (Bax) messenger ribonucleic acid (mRNA) (**Fig. 3A**) and protein (**Figs. 3C and 3D**) in the NE group ($P = 0.0003$ and $P = 0.0001$, respectively), Rd group ($P = 0.0274$ and $P = 0.0002$, respectively), and Vehl group (both, $P = 0.0001$) were significantly higher than those in the Con group, whereas Bcl-2 mRNA (**Fig. 3A**) and protein (**Figs. 3C and 3E**) in the NE group ($P = 0.0002$ and $P = 0.0001$, respectively), Rd group ($P = 0.0130$ and $P = 0.0152$, respectively), and Vehl group ($P = 0.0002$ and $P = 0.0183$, respectively) was significantly lower than that in the Con group. The levels of Bax mRNA, Bax protein, Bcl-2 mRNA, and Bcl-2 protein content in the Rd group were significantly lower than those of the NE group ($P = 0.0157$, $P = 0.0256$, $P = 0.0240$ and $P = 0.0205$, respectively) and Vehl group (P = 0.0037, $P = 0.0187$, $P = 0.0181$, and $P = 0.0106$, respectively).

Effect of GSRd on the gene and protein expression of SIRT1 and PGC-1α in the cochleae of guinea pigs

The mRNA content (**Fig. 3B**) and protein content (**Figs. 3F and 3G**) of SIRT1 in the NE group ($P = 0.0003$ and $P = 0.0001$, respectively), Rd group ($P = 0.0192$ and $P = 0.0015$, respectively) and Vehl group ($P = 0.0003$ and $P = 0.0001$, respectively) were significantly lower than those of the Con group, whereas they were significantly higher in the Rd group than in the NE group ($P = 0.0255$ and $P = 0.0111$, respectively) and Vehl group ($P = 0.0221$ and $P = 0.0173$, respectively). The mRNA content (**Fig. 3B**) and protein content (**Figs. 3F and 3H**) of PGC-1α likewise showed a similar relationship between groups: NE group ($P = 0.0004$ and $P = 0.0001$, respectively), Rd group ($P = 0.0272$ and $P = 0.0003$, respectively), and Vehl group ($P = 0.0006$ and $P = 0.0001$, respectively), compared to the Con group; NE group ($P = 0.0246$ and $P = 0.0101$, respectively) and Vehl group ($P = 0.0454$ and 0.0137, respectively), compared to the Rd group.

GSRd reduced the expression of free radicals in the cochleae of guinea pigs

The common indices of the free radical level test are 4-hydroxy-4-hydroxynonenal (4-HNE) (i.e., an ROS marker) and 3-nitrotyrosine (3-NT) (i.e., a reactive nitrogen species [RNS] marker). In this experiment, 4-HNE was displayed with red fluorescence, 3-NT was displayed with green fluorescence, 4,6-diamino-2-phenylindole (DAPI) staining nucleus was displayed with blue fluorescence, and merge was synthesized in the three colors (**Fig. 4A**). Only a small amount of 4-HNE and 3-NT was expressed in the Con group. Following the noise stimulation, the expression of 4-HNE (**Fig. 4B**) and 3-NT (**Fig. 4C**) was significantly increased in the NE group ($P = 0.0001$) and Vehl group ($P = 0.0001$) and was primarily located in the organ of Corti. The immunofluorescence expression of 4-HNE and 3-NT was decreased significantly in the Rd group ($P = 0.0002$).

GSRd downregulated the level of oxidative stress in the cochleae of guinea pigs

The SOD levels in the NE, Rd, and Vehl groups, compared to the Con group, were decreased by 46.25% ($P = 0.0001$), 22.71% ($P = 0.0122$), and 47.35% ($P = 0.0001$), respectively (**Fig. 5A**). The MDA levels in the NE, Rd, and Vehl groups were increased by 3.30 ($P = 0.0009$), 1.60 ($P = 0.0466$), and 3.53 ($P = 0.0006$) times, respectively, (**Fig. 5B**). The GSH-Px levels in the NE, Rd, and Vehl groups were downregulated by 72.06% ($P = 0.0001$), 39.67% ($P = 0.0027$), and 72.64% ($P = 0.0001$), respectively (**Fig. 5C**). Compared to the NE

and the Vehl groups, the Rd group had significantly increased SOD levels ($P = 0.0099$ and $P = 0.0076$, respectively) and GSH-Px levels ($P = 0.0090$ and $P = 0.0082$, respectively), and had significantly decreased MDA levels following noise stimulation ($P = 0.0430$ and $P = 0.0232$ respectively).

Discussion

In this study, we tested our hypothesis that GSRd supplementation would attenuate NIHL via regulating oxidative stress and apoptosis, mediated by the SIRT1/PGC-1α signaling pathway. Our results suggested that GSRd can alleviate hair cell loss and free radical production in the cochleae of guinea pigs. The possible mechanism may involve the activation of the SIRT1/PGC-1α signaling pathway, the upregulation of SIRT1/PGC-1α expression, increased SOD and GSH-Px activity, and decreased MDA level, which enhances the antioxidant capacity of the auditory system and hence reduces peripheral auditory system damage. The protective effect of GSRd on cochlear hair cell damage via the SIRT1/PGC-1α signaling pathway in guinea pigs are shown in **Fig. 6**.

Our results are consistent with previous findings indicating that GSRd can scavenge free radicals, exert the effects of anti-oxidation, antiaging, and analgesia [43], and that it has a certain protective effect to some extent on the cardiovascular system [44, 45], kidneys [46], immune system [47], and nervous system [48–51]. Ginsenosides (GSs) are the main active components of *Panax ginseng, Panax quinquefolium*, and *Panax notoginseng*. More than 50 types of GS monomers have been isolated and extracted from ginseng plants [52]. The separation of effective monomers from GS is helpful in clarifying its pharmacological effects. Among all GS monomers, Rb1, Rb2, Rc, Re, and Rg1 account for more than 80% of the total saponins, and are thus termed the main saponins. Rd, Rg3, Rh2, and other GS monomers are rare, although their pharmacological efficacy are better than those of the main saponins.

GSRd is a monomer extract of total saponins, which belongs to the protopanaxadiol type structure. Its molecular formula is $C_{48}H_{82}O_{18}\cdot 3H_2O$ and its molecular weight is 1001 Da. GSRd has high fat solubility, easy diffusion, and permeation through biofilm, but has poor water solubility [53]. GSRd has two glycosyl groups on C-3, which is the pharmacological basis of its antioxidant activity [54]. GSRd is a rare saponin monomer, which is low in ginseng and high in *Panax notoginseng* [55]. Intestinal enzymes can metabolize the main saponins Rb1 and Rc into Rd; therefore, Rd is one of the main forms of absorption and utilization of main saponins in the intestine after metabolism [56, 57]. Among the more than 50 types of GS, GSRd is the main active ingredient in many pharmacological actions of *Panax ginseng*.

Our experimental results showed that GSRd treatment may have otoprotective effects by regulating the apoptosis pathway and oxidative stress. Following noise stimulation, the peripheral auditory system is first damaged, including mechanical damage to the inner ear and a series of metabolic damage. The main manifestation of the mechanical and metabolic damage is high-frequency hearing loss. Results from previous research show that, after noise stimulation, the expression of activated Caspase-3 and Bax in the cochlea increases significantly, whereas the expression level of Bcl-2 decreases significantly, thereby resulting in a significant decrease in the Bcl-2/Bax ratio [58]. This finding is consistent with our

results. In addition, excessive ROS and lipid peroxidation were stimulated in the inner ears. The aldehyde products are thus produced and may continue to contribute to the destruction of the normal physiological activities of hair cells, including 4-HNE, which form cross-links with proteins and nucleic acids.

The 4-HNE level is closely associated with oxidative stress, apoptosis, and inflammation, and is considered a marker of ROS. In addition, excessive RNS stimulated by noise nitrify the free tyrosine or tyrosine residues in the protein, thereby resulting in the formation of 3-NT. It attacks the normal structure of the protein, affects its normal physiological function, and causes cell damage, which is a marker of RNS. GSRd treatment downregulated the expression of Bax and free radical markers such as 4-HNE and 3-NT and upregulated the expression of Bcl-2, thereby reducing the level of apoptosis and oxidative stress in the inner ear. Considering the pathogenic mechanisms underlying NIHL, which is associated with ROS, the aforementioned findings suggest that GSRd has protective therapeutic effects against NIHL by regulating the level of oxidative stress in the cochleae.

In this experiment, we observed that the damage to the third-row outer hair cells was the most severe, whereas the damage to inner hair cells was relatively mild. Ren et al. [59] believe that this result may be attributable to the location. Third-row outer hair cells are in the center of the basilar membrane where the largest vibration amplitude occurs. However, the inner hair cells are on the edge of the bony spiral lamina, which is affected by less vibration from the basilar membrane.

SEM revealed that GSRd may improve the lodging and loss of the cilia of hair cells, but the results of basilar membrane preparation were not significantly different between the NE and Vehl groups. We concluded that the abnormal morphology of the cilia and ultrastructural changes in the hair cells generally occurred after noise stimulation. Only when the damage factors reached a certain degree did death and loss of hair cells occur and manifest in the basilar membrane preparation [60].

SIRT1 can activate the antioxidant pathway and significantly reduce ROS levels [61]. Xiong et al. [22] explored SIRT1 expression in the cochlea and found that it was primarily expressed in the spiral ganglion neurons, outer hair cells, inner hair cells, and some supporting cells. A small amount of SIRT1 was expressed in the vascular stria of the lateral wall of the cochlea. The expression of SIRT1 was less pronounced in the outer hair cells than in the inner hair cells [62]. Previous studies have shown that SIRT1 has a protective effect on AHL-induced cochlear damage by activating downstream PGC-1α signaling [63]. Previous publications from our laboratory also indicated that GSRd can ameliorate auditory cortex damage of the central auditory system associated with military aviation noise-induced hearing loss by activating the SIRT1/PGC-1α signaling pathway [35]. Considering the similarities in the pathogenesis between NIHL and AHL, we hypothesized that the upregulation of the SIRT1/PGC-1α signaling pathway also has a role in the otoprotective effects of GSRd on the peripheral auditory system. Our results showed that the mRNA and protein levels of SIRT1/PGC-1α in the cochlea of guinea pigs were downregulated after noise stimulation, which indicated that they may be involved in the noise-induced damage in the inner ear. Moreover, GSRd can upregulate the SIRT1/PGC-1α signaling pathway, which helps to maintain the oxidative balance of the peripheral auditory system, thereby exerting its otoprotective effects.

Conclusions

Our results suggested that GSRd may improve damage to the peripheral auditory system of guinea pigs, caused by military helicopter noise, by activating the SIRT1/PGC-1α signaling pathway. Further studies on the dose-response curve of GSRd in the treatment of NIHL and the therapeutic effect of GSRd after prolonged noise stimulation are recommended. We also recommend further investigation to determine whether GSRd directly regulates oxidative stress levels by regulating SOD and MDA activity, or indirectly regulates these parameters through other signaling pathways.

Abbreviations

ABR, auditory brainstem response; AHL, age-related hearing loss; Bcl-2, B-cell lymphoma-2; Bax, Bcl-2 associated X protein; DAPI, 4,6-diamino-2-phenylindole; GO, gene ontology; GSH-Px, glutathione peroxidase; GSRd, ginsenoside Rd; 4-HNE, 4-hydroxy-4-hydroxynonenal; IgG, immunoglobulin G; MDA, malondialdehyde; NIHL, noise-induced hearing loss; PBS, phosphate-buffered saline; PBST, phosphate-buffered saline-Tween; PGC-1α, proliferator-activated receptor-gamma coactivator 1α; RNA, ribonucleic acid; RNS, reactive nitrogen species; ROS, reactive oxygen species; SEM, scanning electron microscopy; SIRT, Sirtuin1; SOD, superoxide dismutase; TUNEL, terminal dUTP nick end labeling

Declarations

Ethical Approval and Consent to participate

All experimental procedures were approved by the Animal Ethics Committee of our university.

Consent for publication

Not applicable.

Availability of data and materials

All data generated or analyzed during this study are available from the corresponding author on reasonable request. All materials are commercially available.

Competing interests

The authors declare no conflicts of interest.

Funding

This work was supported by grants from the Major Military Project (grant number AWS14L009) and Key Researcher and Development Plan in Shaanxi (grant number 2018SF-252).

Authors’ contributions

CXM, LYH, CYM, and WXC conceived and designed the experiment methods. CXM and LYH drafted the manuscript. JSF performed bioinformatic analysis. CXM and LCC performed phalloidin staining, SEM observation RT-qPCR, and western blot analysis. JSF and XXM performed TUNEL staining. LYH and LP performed immunofluorescence staining for 4-HNE and 3-NT. XXM and LP examined SOD, MDA, and GSH-Px levels. CXM, JSF, and LCC conducted the statistics. CXM and JSF revised the manuscript. WXC, CYM, and ZM take responsibility for the integrity of the data and the accuracy of data analysis.

Acknowledgements

Our deepest gratitude goes to colleagues from College of Otolaryngology & Head and Neck Surgery, Chinese PLA General Hospital, led by Prof. Shiming-Yang and Department of Otolaryngology, Xijing Hospital, led by Prof. Jianhua-Qiu for their valuable technical support.

Authors' information

[1] Department of Aerospace Hygiene, School of Aerospace Medicine, Air Force Medical University, Xi’an, China. [2] Medical School of Chinese PLA, Beijing, China. [3] College of Otolaryngology and Head and Neck Surgery, Chinese PLA General Hospital; National Clinical Research Center for Otolaryngologic Diseases; State Key Lab of Hearing Science, Ministry of Education; Beijing Key Lab of Hearing Impairment Prevention and Treatment, Beijing, China.[4] Center of Clinical Aerospace Medicine, School of Aerospace Medicine, Key Laboratory of Aerospace Medicine of Ministry of Education, Air Force Medical University, Xi’an, China.[5] Department of Aviation Medicine, The First Affiliated Hospital of Air Force Military Medical University, Xi’an, China.[6] Research Center for Tissue Repair and Regeneration Affiliated to the Medical Innovation Research Department and 4th Medical Center, Chinese PLA General Hospital, Beijing, China.

References

1. Ding T, Yan A, Liu K. What is noise-induced hearing loss? Br J Hosp Med (Lond). 2019;80(9):525–9.
2. Kowalski TJ, Pawelczyk M, Rajkowska E, Dudarewicz A, Sliwinska-Kowalska M. Genetic variants of CDH23 associated with noise-induced hearing loss. Otology neurotology: official publication of the American Otological Society American Neurotology Society [and] European Academy of Otology Neurotology. 2014;35(2):358–65.

3. Wu Y, Ni J, Qi M, Cao C, Shao Y, Xu L, Ma H, Yang L. Associations of genetic variation in CASP3 gene with noise-induced hearing loss in a Chinese population: a case-control study. Environmental health: a global access science source. 2017;16(1):78.
4. Yu P, Jiao J, Chen G, Zhou W, Zhang H, Wu H, Li Y, Gu G, Zheng Y, Yu Y, et al. Effect of GRM7 polymorphisms on the development of noise-induced hearing loss in Chinese Han workers: a nested case-control study. BMC medical genetics. 2018;19(1):4.
5. Pawelczyk M, Van Laer L, Fransen E, Rajkowska E, Konings A, Carlsson PI, Borg E, Van Camp G, Sliwinska-Kowalska M. Analysis of gene polymorphisms associated with K ion circulation in the inner ear of patients susceptible and resistant to noise-induced hearing loss. Annals of human genetics. 2009;73(Pt 4):411–21.
6. Bielefeld EC. Protection from noise-induced hearing loss with Src inhibitors. Drug Discov Today. 2015;20(6):760–5.
7. Imam L, Hannan SA. Noise-induced hearing loss: a modern epidemic? Br J Hosp Med (Lond). 2017;78(5):286–90.
8. Basta D, Gröschel M, Ernst A. [Central and peripheral aspects of noise-induced hearing loss]. Hno. 2018;66(5):342–9.
9. Henderson D, Bielefeld EC, Harris KC, Hu BH. The role of oxidative stress in noise-induced hearing loss. Ear Hear. 2006;27(1):1–19.
10. Honkura Y, Matsuo H, Murakami S, Sakiyama M, Mizutari K, Shiotani A, Yamamoto M, Morita I, Shinomiya N, Kawase T, et al. NRF2 Is a Key Target for Prevention of Noise-Induced Hearing Loss by Reducing Oxidative Damage of Cochlea. Scientific reports. 2016;6:19329.
11. Tuerdi A, Kinoshita M, Kamogashira T, Fujimoto C, Iwasaki S, Shimizu T, Yamasoba T. Manganese superoxide dismutase influences the extent of noise-induced hearing loss in mice. Neurosci Lett. 2017;642:123–8.
12. Le TN, Straatman LV, Lea J, Westerberg B. Current insights in noise-induced hearing loss: a literature review of the underlying mechanism, pathophysiology, asymmetry, and management options. J Otolaryngol Head Neck Surg. 2017;46(1):41.
13. Maillet A, Pervaiz S. Redox regulation of p53, redox effectors regulated by p53: a subtle balance. Antioxid Redox Signal. 2012;16(11):1285–94.
14. Mercken EM, Mitchell SJ, Martin-Montalvo A, Minor RK, Almeida M, Gomes AP, Scheibye-Knudsen M, Palacios HH, Licata JJ, Zhang Y, et al. SRT2104 extends survival of male mice on a standard diet and preserves bone and muscle mass. Aging Cell. 2014;13(5):787–96.
15. Mitchell SJ, Martin-Montalvo A, Mercken EM, Palacios HH, Ward TM, Abulwerdi G, Minor RK, Vlasuk GP, Ellis JL, Sinclair DA, et al. The SIRT1 activator SRT1720 extends lifespan and improves health of mice fed a standard diet. Cell Rep. 2014;6(5):836–43.
16. Nemoto S, Fergusson MM, Finkel T. SIRT1 functionally interacts with the metabolic regulator and transcriptional coactivator PGC-1{alpha}. J Biol Chem. 2005;280(16):16456–60.

17. Singh CK, Chhabra G, Ndiaye MA, Garcia-Peterson LM, Mack NJ, Ahmad N. The Role of Sirtuins in Antioxidant and Redox Signaling. Antioxid Redox Signal. 2018;28(8):643–61.
18. Andres AM, Stotland A, Queliconi BB, Gottlieb RA. A time to reap, a time to sow: mitophagy and biogenesis in cardiac pathophysiology. J Mol Cell Cardiol. 2015;78:62–72.
19. Kudryavtseva AV, Krasnov GS, Dmitriev AA, Alekseev BY, Kardymon OL, Sadritdinova AF, Fedorova MS, Pokrovsky AV, Melnikova NV, Kaprin AD, et al. Mitochondrial dysfunction and oxidative stress in aging and cancer. Oncotarget. 2016;7(29):44879–905.
20. Oberdoerffer P, Michan S, McVay M, Mostoslavsky R, Vann J, Park SK, Hartlerode A, Stegmuller J, Hafner A, Loerch P, et al. SIRT1 redistribution on chromatin promotes genomic stability but alters gene expression during aging. Cell. 2008;135(5):907–18.
21. Xue T, Wei L, Zha DJ, Qiu JH, Chen FQ, Qiao L, Qiu Y. miR-29b overexpression induces cochlear hair cell apoptosis through the regulation of SIRT1/PGC-1α signaling: Implications for age-related hearing loss. Int J Mol Med. 2016;38(5):1387–94.
22. Xiong H, Dai M, Ou Y, Pang J, Yang H, Huang Q, Chen S, Zhang Z, Xu Y, Cai Y, et al. SIRT1 expression in the cochlea and auditory cortex of a mouse model of age-related hearing loss. Experimental gerontology. 2014;51:8–14.
23. Xiong H, Pang J, Yang H, Dai M, Liu Y, Ou Y, Huang Q, Chen S, Zhang Z, Xu Y, et al. Activation of miR-34a/SIRT1/p53 signaling contributes to cochlear hair cell apoptosis: implications for age-related hearing loss. Neurobiol Aging. 2015;36(4):1692–701.
24. Xiong H, Ou Y, Xu Y, Huang Q, Pang J, Lai L, Zheng Y. Resveratrol Promotes Recovery of Hearing following Intense Noise Exposure by Enhancing Cochlear SIRT1 Activity. Audiol Neurootol. 2017;22(4–5):303–10.
25. Kim HJ, Kim P, Shin CY. A comprehensive review of the therapeutic and pharmacological effects of ginseng and ginsenosides in central nervous system. J Ginseng Res. 2013;37(1):8–29.
26. Kim MY, Cho JY. 20S-dihydroprotopanaxadiol, a ginsenoside derivative, boosts innate immune responses of monocytes and macrophages. J Ginseng Res. 2013;37(3):293–9.
27. Wang Y, Kan H, Yin Y, Wu W, Hu W, Wang M, Li W, Li W. Protective effects of ginsenoside Rg1 on chronic restraint stress induced learning and memory impairments in male mice. Pharmacol Biochem Behav. 2014;120:73–81.
28. Peng L, Sun S, Xie LH, Wicks SM, Xie JT. Ginsenoside Re: pharmacological effects on cardiovascular system. Cardiovasc Ther. 2012;30(4):e183–8.
29. González-Burgos E, Fernández-Moriano C, Lozano R, Iglesias I, Gómez-Serranillos MP. Ginsenosides Rd and Re co-treatments improve rotenone-induced oxidative stress and mitochondrial impairment in SH-SY5Y neuroblastoma cells. Food Chem Toxicol. 2017;109(Pt 1):38–47.
30. Liu JF, Yan XD, Qi LS, Li L, Hu GY, Li P, Zhao G. Ginsenoside Rd attenuates Aβ25-35-induced oxidative stress and apoptosis in primary cultured hippocampal neurons. Chem Biol Interact. 2015;239:12–8.
31. Nabavi SF, Sureda A, Habtemariam S, Nabavi SM. Ginsenoside Rd and ischemic stroke; a short review of literatures. J Ginseng Res. 2015;39(4):299–303.

32. Xu HY, Zhang YQ, Liu ZM, Chen T, Lv CY, Tang SH, Zhang XB, Zhang W, Li ZY, Zhou RR, et al. ETCM: an encyclopaedia of traditional Chinese medicine. Nucleic acids research. 2019;47(D1):D976–82.
33. Szklarczyk D, Santos A, von Mering C, Jensen LJ, Bork P, Kuhn M. STITCH 5: augmenting protein-chemical interaction networks with tissue and affinity data. Nucleic acids research. 2016;44(D1):D380–4.
34. Chen XM, Xue XM, XU J, Deng SL, Chang YM, Wang XC. Effects of a Military Helicopter Noise Exposure on Auditory Function of Guinea Pigs. Space Medicine Medical Engineering. 2019;32:406–11.
35. Chen X, Ji S, Liu Y, Xue X, Xu J, Gu Z, Deng S, Liu C, Wang H, Chang Y, et al. Ginsenoside Rd Ameliorates Auditory Cortex Injury Associated With Military Aviation Noise-Induced Hearing Loss by Activating SIRT1/PGC-1α Signaling Pathway. Frontiers in physiology. 2020;11:788.
36. Qi M, Qiu Y, Zhou X, Tian K, Zhou K, Sun F, Yue B, Chen F, Zha D, Qiu J. Regional up-regulation of NOX2 contributes to the differential vulnerability of outer hair cells to neomycin. Biochem Biophys Res Commun. 2018;500(2):110–6.
37. Sung CM, Kim HC, Cho YB, Shin SY, Jang CH. Evaluating the ototoxicity of an anti-MRSA peptide KR-12-a2. Brazilian journal of otorhinolaryngology. 2018;84(4):441–7.
38. Santi PA, Aldaya R, Brown A, Johnson S, Stromback T, Cureoglu S, Rask-Andersen H. Scanning Electron Microscopic Examination of the Extracellular Matrix in the Decellularized Mouse and Human Cochlea. Journal of the Association for Research in Otolaryngology: JARO. 2016;17(3):159–71.
39. Liu HJ, Jiang XX, Guo YZ, Sun FH, Kou XH, Bao Y, Zhang ZQ, Lin ZH, Ding TB, Jiang L, et al. The flavonoid TL-2-8 induces cell death and immature mitophagy in breast cancer cells via abrogating the function of the AHA1/Hsp90 complex. Acta pharmacologica Sinica. 2017;38(10):1381–93.
40. Tian K, Song Y, Zhou K, Yue B, Qiu Y, Sun F, Wang R, Zha D, Qiu J. Upregulation of HSP60 expression in the postnatal rat cochlea and rats with drug-induced hearing loss. Cell stress chaperones. 2018;23(6):1311–7.
41. Su YT, Guo YB, Cheng YP, Zhang X, Xie XP, Chang YM, Bao JX. **Hyperbaric Oxygen Treatment Ameliorates Hearing Loss and Auditory Cortex Injury in Noise Exposed Mice by Repressing Local Ceramide Accumulation**. *International journal of molecular sciences* 2019, 20(19).
42. Zhang J, Song YL, Tian KY, Qiu JH. Minocycline attenuates noise-induced hearing loss in rats. Neurosci Lett. 2017;639:31–5.
43. Choi SS, Lee JK, Suh HW. Effect of ginsenosides administered intrathecally on the antinociception induced by cold water swimming stress in the mouse. Biol Pharm Bull. 2003;26(6):858–61.
44. Zhang N, An X, Lang P, Wang F, Xie Y. Ginsenoside Rd contributes the attenuation of cardiac hypertrophy in vivo and in vitro. Biomedicine pharmacotherapy = Biomedecine pharmacotherapie. 2019;109:1016–23.
45. Zeng X, Li J, Li Z. Ginsenoside Rd mitigates myocardial ischemia-reperfusion injury via Nrf2/HO-1 signaling pathway. Int J Clin Exp Med. 2015;8(8):14497–504.

46. Ren K, Jin C, Ma P, Ren Q, Jia Z, Zhu D. Ginsenoside Rd alleviates mouse acute renal ischemia/reperfusion injury by modulating macrophage phenotype. Journal of ginseng research. 2016;40(2):196–202.
47. Zhang YX, Wang L, Xiao EL, Li SJ, Chen JJ, Gao B, Min GN, Wang ZP, Wu YJ. Ginsenoside-Rd exhibits anti-inflammatory activities through elevation of antioxidant enzyme activities and inhibition of JNK and ERK activation in vivo. Int Immunopharmacol. 2013;17(4):1094–100.
48. Zhang X, Wang Y, Ma C, Yan Y, Yang Y, Wang X, Rausch WD. Ginsenoside Rd and ginsenoside Re offer neuroprotection in a novel model of Parkinson's disease. American journal of neurodegenerative disease. 2016;5(1):52–61.
49. Liu J, Yan X, Li L, Li Y, Zhou L, Zhang X, Hu X, Zhao G. Ginsenoside Rd Improves Learning and Memory Ability in APP Transgenic Mice. Journal of molecular neuroscience: MN. 2015;57(4):522–8.
50. Liu J, Yan X, Li L, Zhu Y, Qin K, Zhou L, Sun D, Zhang X, Ye R, Zhao G. Ginsennoside rd attenuates cognitive dysfunction in a rat model of Alzheimer's disease. Neurochem Res. 2012;37(12):2738–47.
51. Zhang C, Du F, Shi M, Ye R, Cheng H, Han J, Ma L, Cao R, Rao Z, Zhao G. Ginsenoside Rd protects neurons against glutamate-induced excitotoxicity by inhibiting ca(2+) influx. Cell Mol Neurobiol. 2012;32(1):121–8.
52. Yu SE, Mwesige B, Yi YS, Yoo BC. Ginsenosides: the need to move forward from bench to clinical trials. Journal of ginseng research. 2019;43(3):361–7.
53. Liu ZQ, Luo XY, Liu GZ, Chen YP, Wang ZC, Sun YX. In vitro study of the relationship between the structure of ginsenoside and its antioxidative or prooxidative activity in free radical induced hemolysis of human erythrocytes. J Agric Food Chem. 2003;51(9):2555–8.
54. Yang L, Deng Y, Xu S, Zeng X. In vivo pharmacokinetic and metabolism studies of ginsenoside Rd. Journal of chromatography B Analytical technologies in the biomedical life sciences. 2007;854(1–2):77–84.
55. Karikura M, Tanizawa H, Hirata T, Miyase T, Takino Y: **Studies on absorption**, **distribution**, **excretion and metabolism of ginseng saponins**. **VIII**. **Isotope labeling of ginsenoside Rb2**. *Chemical & pharmaceutical bulletin* 1992, **40**(9):2458–2460.
56. Kim H, Kim JH, Lee PY, Bae KH, Cho S, Park BC, Shin H, Park SG. Ginsenoside Rb1 is Transformed into Rd and Rh2 by Microbacterium trichothecenolyticum. J Microbiol Biotechn. 2013;23(12):1802–5.
57. Ye R, Han J, Kong X, Zhao L, Cao R, Rao Z, Zhao G. Protective effects of ginsenoside Rd on PC12 cells against hydrogen peroxide. Biol Pharm Bull. 2008;31(10):1923–7.
58. Jia H, Yu Z, Ge X, Chen Z, Huang X, Wei Y. Glucocorticoid-induced leucine zipper protects noise-induced apoptosis in cochlear cells by inhibiting endoplasmic reticulum stress in rats. Med Mol Morphol. 2020;53(2):73–81.
59. Ren T. Longitudinal pattern of basilar membrane vibration in the sensitive cochlea. Proc Natl Acad Sci USA. 2002;99(26):17101–6.
60. Ding DL. **Science of the inner ear**. *China science & technology press* 2010.

61. Seo JS, Moon MH, Jeong JK, Seol JW, Lee YJ, Park BH, Park SY. SIRT1, a histone deacetylase, regulates prion protein-induced neuronal cell death. Neurobiol Aging. 2012;33(6):1110–20.
62. Takumida M, Takumida H, Katagiri Y, Anniko M. Localization of sirtuins (SIRT1-7) in the aged mouse inner ear. Acta oto-laryngologica. 2016;136(2):120–31.
63. Xue T, Wei L, Zha DJ, Qiu JH, Chen FQ, Qiao L, Qiu Y. miR-29b overexpression induces cochlear hair cell apoptosis through the regulation of SIRT1/PGC-1alpha signaling: Implications for age-related hearing loss. Int J Mol Med. 2016;38(5):1387–94.

Tables

Table 1
Single gene enrichment analysis of GSRd

#Pathway ID	Pathway description	False discovery rate	Matching proteins in your network (labels)
GO.0034599	Cellular response to oxidative stress	0.00000000727	EP300, FoxO1, FoxO3, KAT2B, **PGC-1α, SIRT1**, TP53
GO.0071453	Cellular response to oxygen levels	0.000124	EP300, FoxO1, **PGC-1α, SIRT1**
GO.0042981	Regulation of apoptotic process	0.000201	EP300, FoxO1, FoxO3, KIAA1967, **PGC-1α, SIRT1**, TP53
GO.1901701	Cellular response to oxygen-containing compound	0.000201	EP300, FoxO1, FoxO4, KAT2B, **PGC-1α, SIRT1**
GO.0009719	Response to endogenous stimulus	0.000216	FoxO1, FoxO3, FoxO4, KAT2B, **PGC-1α, SIRT1**, TP53
GO.0043066	Negative regulation of apoptotic process	0.000243	EP300, FoxO1, KIAA1967, **PGC-1α, SIRT1**, TP53
GO.0042127	Regulation of cell proliferation	0.00026	FoxO1, FoxO3, FoxO4, KAT2B, **PGC-1α, SIRT1**, TP53
GO.1901214	Regulation of neuron death	0.000731	FoxO3, **PGC-1α, SIRT1**, TP53
GO.0010468	Regulation of gene expression	0.00577	EP300, FoxO3, KAT2B, KIAA1967, **PGC-1α, SIRT1**, TP53, XRCC6
GO.0032922	Circadian regulation of gene expression	0.0194	**PGC-1α, SIRT1**

EP300:E1A binding protein p300; FoxO:Forkhead box O; KAT2:K(lysine) acetyltransferase 2B; PGC-1α:Peroxisome proliferator-activated receptor gamma, coactivator 1 alpha; XRCC6:X-ray repair complementing defective repair in Chinese hamster cells 6.

Table 2
Distribution of cochlear specimens of guinea pigs

Experiment	Number	Experiment	Number
Surface preparation of basilar membrane	3	Scanning electron microscope	3
Section staining	3	Western blot	6
RT-qPCR	3	SOD、MDA、GSH-Px analysis	6

Table 3
Sequences of primers used in this study

Gene Name	Forward (5'-3')	Reverse (5'-3')
GAPDH	GGAAGCTGTGGCGTGATGGC	TTCTCCAGGCGGCAGGTCAG
Bax	TCGCTGATGGCAACTTCAACTGG	GGCGGTCTCGGAGGAAGTCTAG
Bcl-2	CCAAGACTTCGCTGAGATGTCCAG	GGCGATGTTGTCCACCAGAGG
SIRT1	CGTTGGAACAAGTTGCAGGAATCC	TCCTCGTACAGCTTCACAGTCAAC
PGC-1α	GACACAACACGGACAGAACTGAGG	GCATCACAGGTGTAACGGTAGGTG

Figures

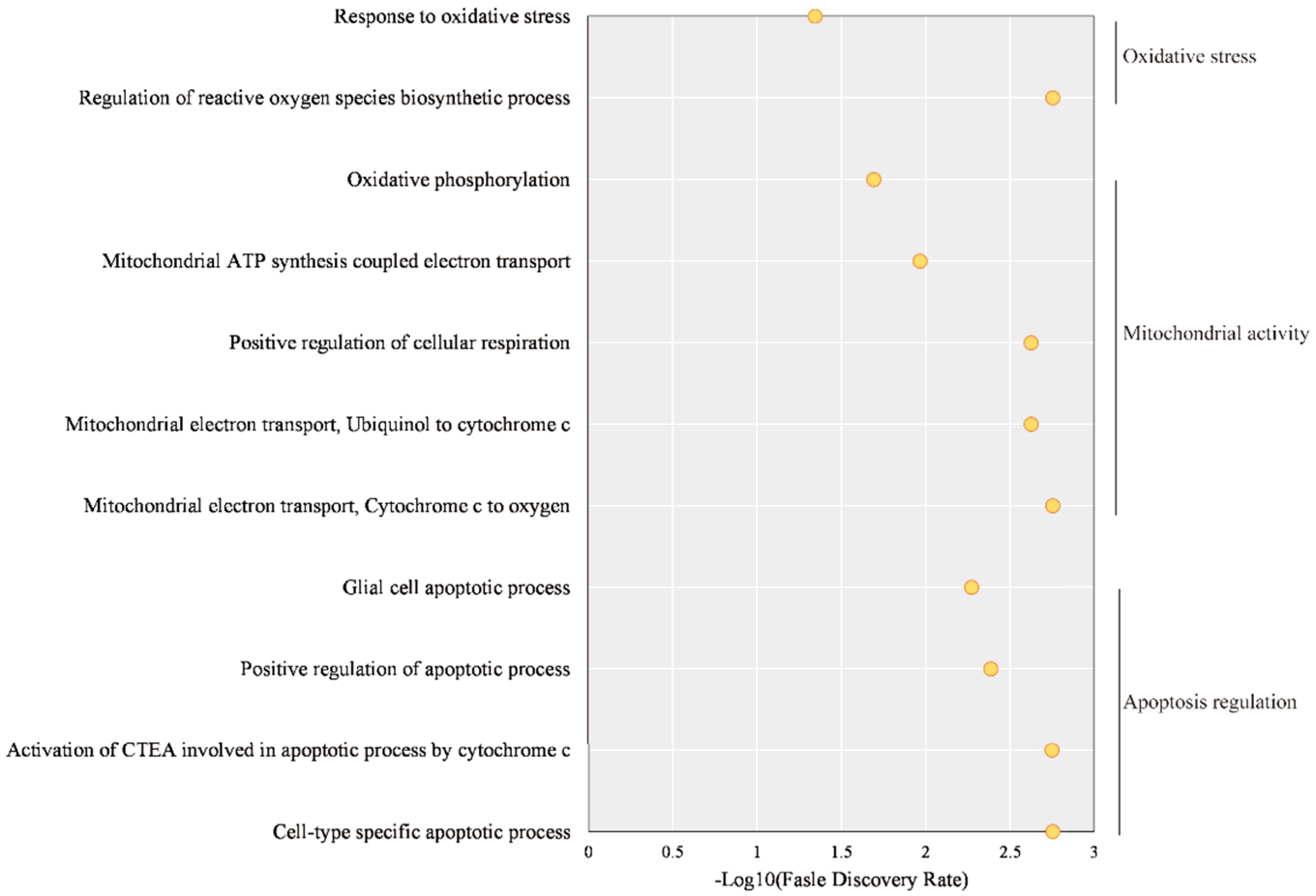

Figure 1

GO enrichment analysis about GSRd via STITCH database. CETA, cysteine-type endopeptidase activity

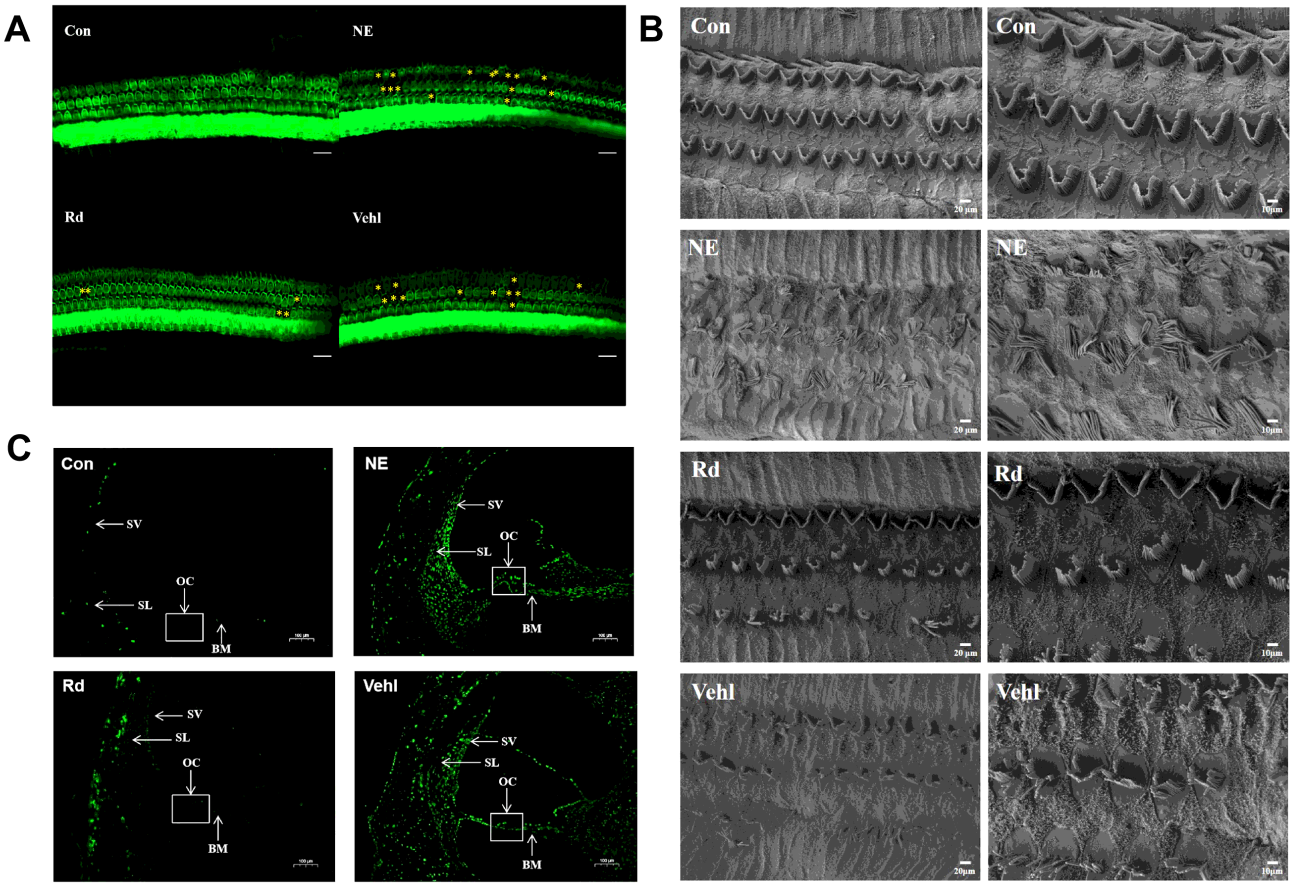

Figure 2

GSRd ameliorated damage and apoptotic levels of cochlear hair cells of guinea pigs. Laying of hair cells (A) , SEM observation (B) and TUNEL staining (C) of the basilar membrane of the four groups after noise stimulation. The “*” symbol indicates the loss of hair cells. OC: organ of Corti ; BM: basilar membrane; SV: stria vascularis; SL: spiral ligament. (A) Scale bar = 50 μm.(B) Scale bar (left) = 20 μm. Scale bar (right) = 10 μm.(C) Scale bar=100 μm.

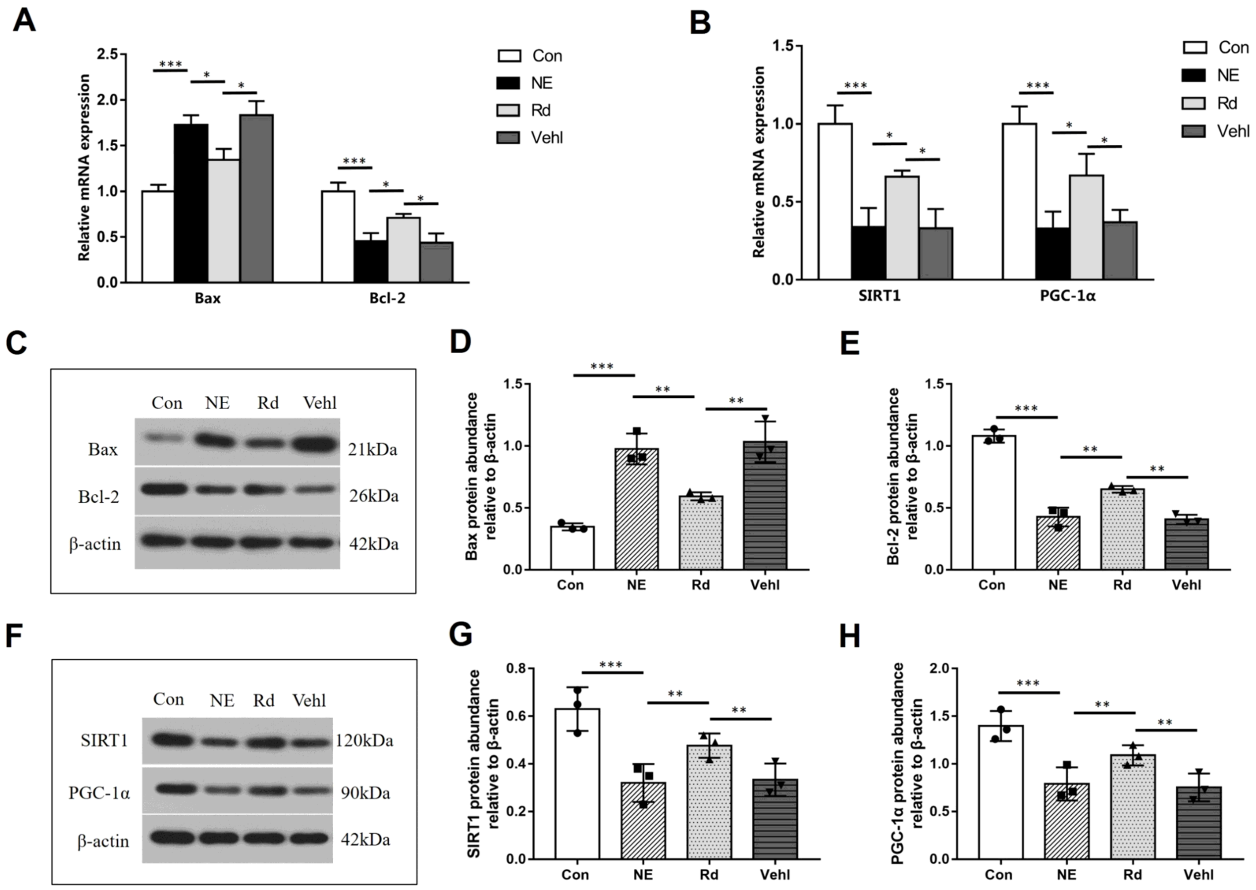

Figure 3

Effect of GSRd on the expression of apoptotic and ROS-related factors in the cochleac of guinea pigs. RT-qPCR (A, B) and Western blotting analysis (C-H) showing the levels of Bax, Bel-2, SIRT-1 and PGC-1α in the cochleae of the four groups after noise stimulation. The values are presented as the means ± SE. n= 3 in each group. *P< 0.05, **P< 0.01, *** < 0.001.

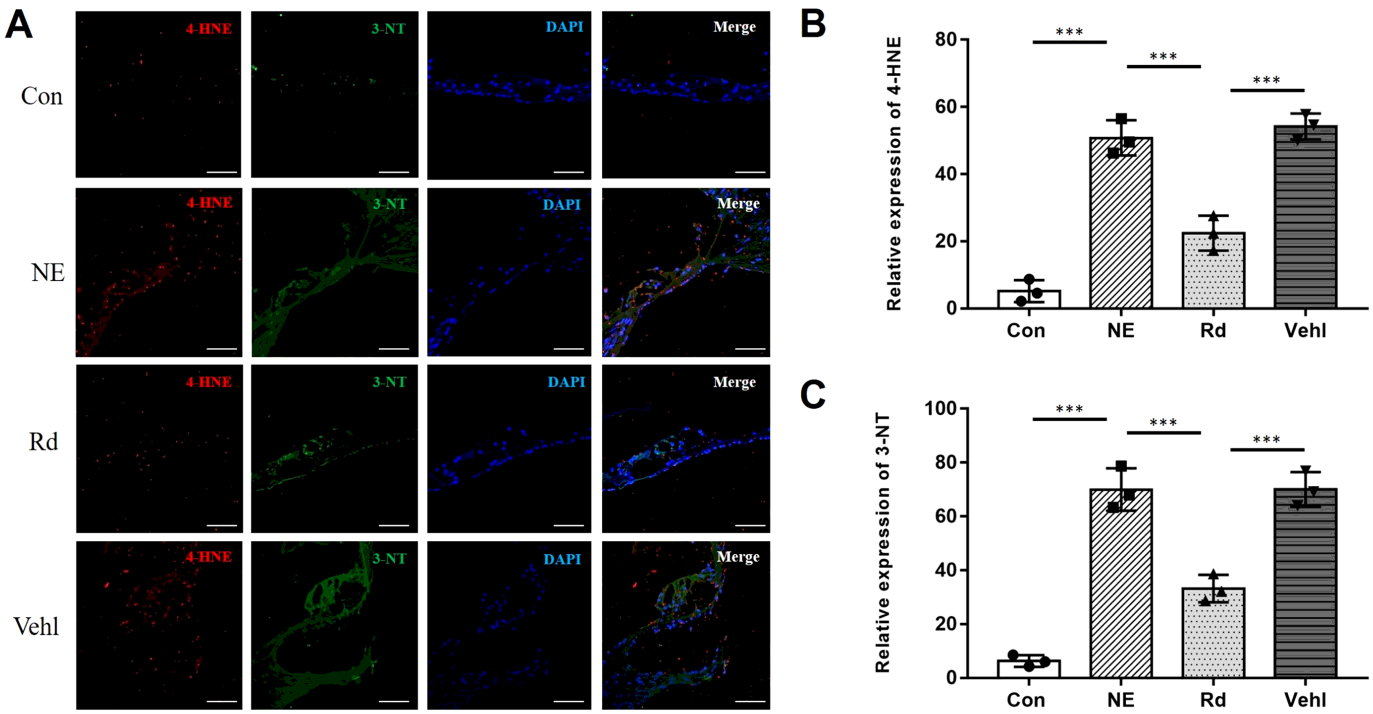

Figure 4

GSRd reduced the expression of free radicals in the cochleae of guinea pigs. Immunofluorescence (IF) staining of 4-HNE and 3-NT in the cochleae of the four groups after noise stimulation. (A) Original images of IF staining of 4-HNE and 3-NT in the cochleae of the four groups after noise stimulation. DAPI staining indicates the location of the nucleus. Scale bar = 200 μm. (B.C) Summarized data of IF staining of 4-HNE and 3-NT in the cochleae of the four groups afer noise stimulation, The values are presented as the means ± SE. n= 3 in cach group. ***P < 0.001.

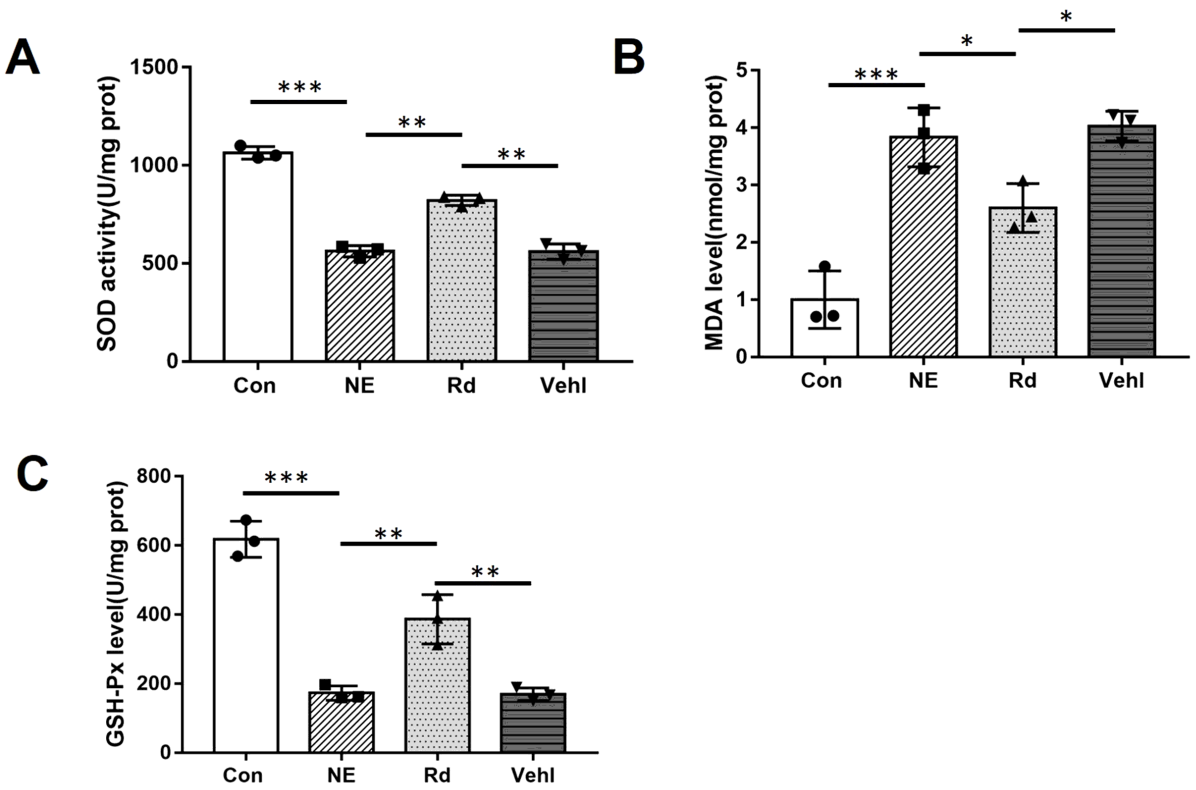

Figure 5

GSRd downregulated the level of oxidative stress in the cochleae of guinea pigs. SOD activity (A), MDA (B) and GSH-Px levels (C) in the cochleae of guinea pigs of the four groups after noise stimulation.The values are presented as the means ± SE. n= 3 in each colorimetric assay. *P < 0.05, **P< 0.01, ***P < 0.001.

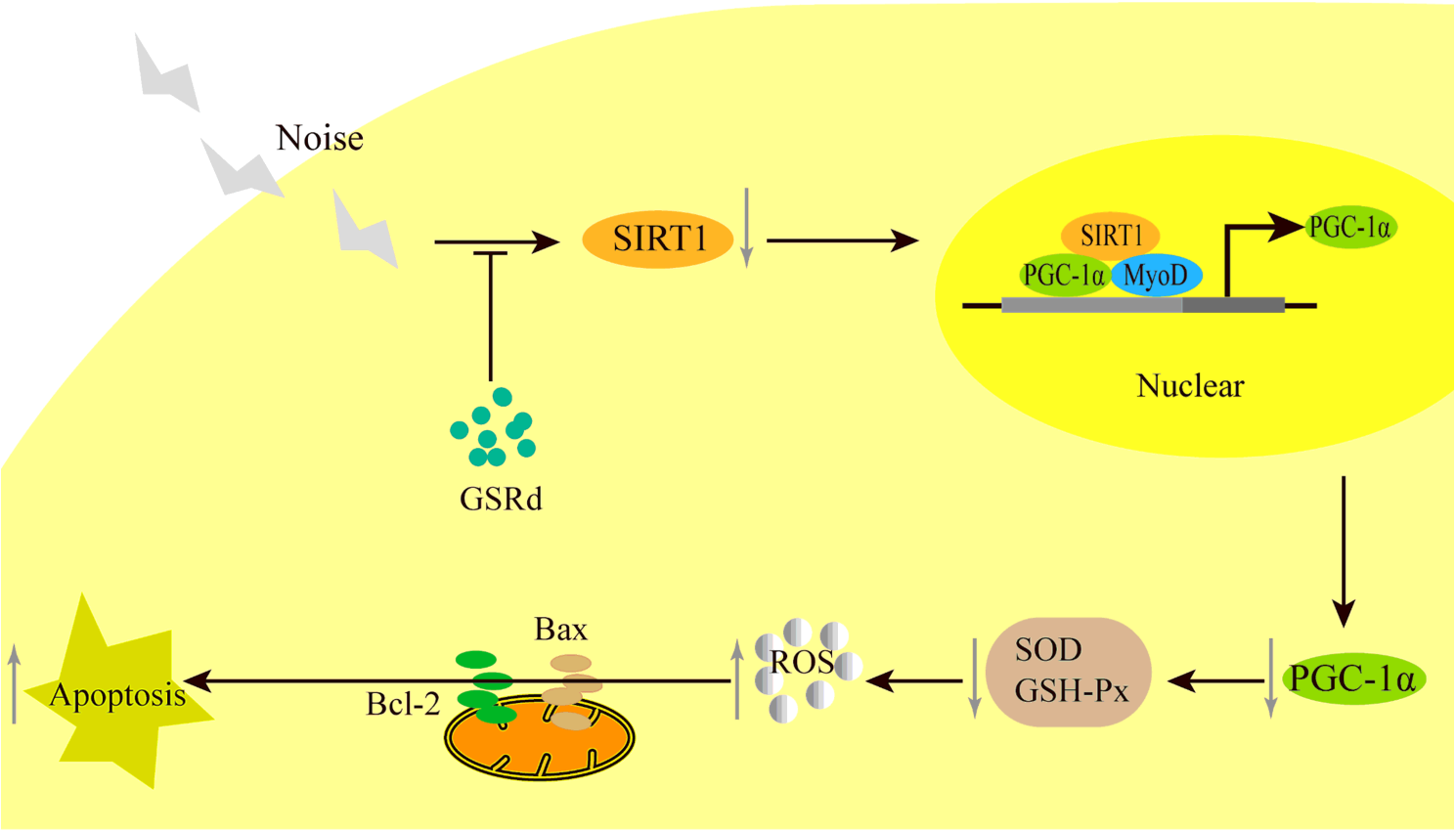

Figure 6

Protective effect of GSRd on cochlear hair cell damage via SIRT1/PGC-1α signaling pathway in guinea pigs.

Supplementary Files

This is a list of supplementary files associated with this preprint. Click to download.

- Supplementaryfigure1.tif